Inter- and Intraspecific Variation in the *Artibeus* species complex demonstrates size and shape partitioning among species

Brandon P Hedrick [Corresp. 1]

[1] Cell Biology and Anatomy, Louisiana State University Health Sciences Center- New Orleans, New Orleans, United States

Corresponding Author: Brandon P Hedrick
Email address: bphedrick1@gmail.com

Neotropical leaf-nosed bats (family Phyllostomidae) are one of the most diverse mammalian families and *Artibeus* spp. is one of the most speciose phyllostomid genera. In spite of their species diversity, previous work on *Artibeus* crania using linear morphometrics has uncovered limited interspecific variation. This dearth of shape variation suggests that differences in cranial morphology are not contributing to niche partitioning across species, many of which are often found in sympatry. Using two-dimensional geometric morphometric methods on crania from eleven species from the *Artibeus* species complex, the current study demonstrates substantial cranial interspecific variation, sexual size and shape dimorphism, and intraspecific geographic variation. The majority of species were shown to have a unique size and shape, which suggests that each species may be taking advantage of slightly different ecological resources. Further, both sexual size and shape dimorphism were significant in the *Artibeus* species complex. Male and female *Artibeus* are known to have sex specific foraging strategies, with males eating near their roosts and females feeding further from their roosts. The presence of cranial sexual dimorphism in the *Artibeus* species complex, combined with previous work showing that different fruit size and hardness is correlated with different cranial shapes in phyllostomids, indicates that the males and females may be utilizing different food resources, leading to divergent cranial morphotypes. Additional field studies will be required to confirm this emergent hypothesis. Finally, significant geographical shape variation was found in a large intraspecific sample of *Artibeus lituratus* crania. However, this variation was not correlated with latitude and instead may be linked to local environmental factors. Additional work on ecology and behavior in the *Artibeus* species complex underlying the morphological variation uncovered in this study will allow for a better understanding of how the group has reached its present diversity.

1 **Inter- and Intraspecific Variation in the *Artibeus* species complex demonstrates size and**
2 **shape partitioning among species**

4 Brandon P. Hedrick[1]
5 [1]Department of Cell Biology and Anatomy, School of Medicine, Louisiana State University Health
6 Science Center, New Orleans, LA 70112, USA
7
8 Corresponding Author:
9
10 Brandon P. Hedrick
11
12 Email address: bphedrick1@gmail.com

Abstract:

16 Neotropical leaf-nosed bats (family Phyllostomidae) are one of the most diverse mammalian
17 families and *Artibeus* spp. is one of the most speciose phyllostomid genera. In spite of their
18 species diversity, previous work on *Artibeus* crania using linear morphometrics has uncovered
19 limited interspecific variation. This dearth of shape variation suggests that differences in cranial
20 morphology are not contributing to niche partitioning across species, many of which are often
21 found in sympatry. Using two-dimensional geometric morphometric methods on crania from
22 eleven species from the *Artibeus* species complex, the current study demonstrates substantial
23 cranial interspecific variation, sexual size and shape dimorphism, and intraspecific geographic
24 variation. The majority of species were shown to have a unique size and shape, which suggests
25 that each species may be taking advantage of slightly different ecological resources. Further,
26 both sexual size and shape dimorphism were significant in the *Artibeus* species complex. Male
27 and female *Artibeus* are known to have sex specific foraging strategies, with males eating near
28 their roosts and females feeding further from their roosts. The presence of cranial sexual
29 dimorphism in the *Artibeus* species complex, combined with previous work showing that
30 different fruit size and hardness is correlated with different cranial shapes in phyllostomids,
31 indicates that the males and females may be utilizing different food resources, leading to
32 divergent cranial morphotypes. Additional field studies will be required to confirm this emergent
33 hypothesis. Finally, significant geographical shape variation was found in a large intraspecific
34 sample of *Artibeus lituratus* crania. However, this variation was not correlated with latitude and
35 instead may be linked to local environmental factors. Additional work on ecology and behavior
36 in the *Artibeus* species complex underlying the morphological variation uncovered in this study
37 will allow for a better understanding of how the group has reached its present diversity.
38
39 Los murciélagos neotropical de hoja nasal (filostómidos) son una de las familias mamíferas más
40 diversas y *Artibeus* spp. es el género filostómido con más especies. A pesar de su riqueza de
41 especies, trabajos anteriores sobre el cráneo *Artibeus* usando morfometría lineal han descubierto
42 limitantes a la variación interespecífica. Esta falta de variación de forma sugiere la ausencia de
43 partición de nicho en todas las especies, muchas de las cuales con frecuencia se encuentran en
44 simpatría. Usando métodos geométricos morfométricos bidimensionales en una muestra grande
45 de cráneos de once especies del complejo de especies *Artibeus* (*Artibeus* y *Dermanura*), el
46 estudio actual demuestra una variación craneal interespecífica, dimorfismo sexual en tamaño y
47 forma y variación geográfica intraespecífica. La mayoría de las especies mostraron un tamaño y
48 forma únicos, lo cual sugiere que cada especie aprovecha nichos ligeramente distintos. Asimismo,
49 el dimorfismo sexual en tamaño y forma fue significativo en el complejo de especies *Artibeus*.
50 Los *Artibeus* machos y hembras tienen estrategias de forrajeo específicos al sexo, ya que los
51 machos comen cerca de sus perchas y las hembras comen lejos de sus perchas. La presencia de
52 dimorfismo sexual craneal en el complejo de especies *Artibeus*, al igual que trabajos anteriores
53 que muestran que diferentes tamaños y durezas de fruta están relacionados con las diferentes
54 formas craneales de filostómidos, indican que los machos y las hembras pueden estar utilizando
55 recursos de alimento diferentes, llevando a morfotipos craneales divergentes. Por último, se
56 encontró una considerable variación de tamaño geográfica en una muestra grande intraespecífica
57 de cráneos de *Artibeus lituratus*. No obstante, esta variación no estuvo relacionada con la latitud
58 y en cambio puede estar ligada a los factores ambientales locales. Trabajo adicional sobre la
59 ecología y comportamiento del complejo de especies *Artibeus* subyacentes a la variación

60 morfológica descubierta en este estudio hará posible un mejor entendimiento acerca de cómo el
61 grupo ha logrado su diversidad actual.
62
63 **Key Words:** Phyllostomidae, Neotropical leaf-nosed bats, Chiroptera, geometric morphometrics
64
65 **Introduction**
66   Of the nearly 6500 species of extant mammals, more than 60% are rodents or bats
67 (Burgin et al., 2018). Numerous factors such as novel functional innovation (the ever-growing
68 teeth of rodents, wings of bats) and the repeated evolution of successful locomotor and foraging
69 modes have led these mammal groups to diversify across the globe (Arita and Fenton, 1997; Kay
70 and Hoekstra, 2009; Morales et al., 2019; Hedrick et al., 2020). One family of bats, the
71 Neotropical leaf-nosed bats (Family Phyllostomidae) are often considered to represent an
72 adaptive radiation and have diversified into more dietary niches than any other mammalian
73 family (Freeman, 2000; Jones et al., 2005; Dumont et al., 2012; 2014; Shi & Rabosky, 2015).
74 Ancestrally insectivorous, phyllostomids have expanded into also eating fruit, nectar, blood, and
75 leaves. Members of the Phyllostomidae are widespread throughout the Neotropics and are found
76 in southern North America and throughout Central and South America. In spite of their dietary
77 breadth and expansion across a wide geographical range, all phyllostomids are relatively small
78 bats (7–200 g). How phyllostomids, and bats more generally, have been able to achieve their
79 species diversity, especially when such a large number of species in the tropics live in sympatry,
80 is an open question.
81   *Artibeus* is one of the most speciose genera in the Phyllostomidae (Lim et al., 2008) and
82 has been considered to be a model for understanding bat diversification (Ferreira et al., 2014).
83 The *Artibeus* species complex is composed of two groups, colloquially termed small *Artibeus*
84 and large *Artibeus*, which are sometimes split at the genus level into *Dermanura* spp.
85 (corresponding to small *Artibeus*) and *Artibeus* spp. (corresponding to large *Artibeus*) (Redondo
86 et al., 2008). All members of the *Artibeus* species complex eat fruit, subsisting primarily on figs,
87 and the species complex spans geographically from Mexico to Argentina. The *Artibeus* species
88 complex has also been shown to have relatively limited morphological variation (Balseiro et al.,
89 2009; Marchán-Rivadeneira et al., 2010). However, size is an important discriminator among
90 species (Ortega & Castro-Arellano, 2001; Larsen et al., 2010) and may be one of the main
91 factors allowing the *Artibeus* species complex to spread into separate niches. A better
92 understanding of interspecific and intraspecific variation within the *Artibeus* species complex
93 will grant further insight into not only the radiation of the Phyllostomidae, but also the
94 diversification of mammalian species that live in sympatry.
95   Morphometrics is commonly used to quantify morphological shape for comparison with
96 ecological variables to better understand how and why morphological variation within a group
97 exists (Samuels & Van Valkenburgh, 2008; Moore et al., 2015; Vander Linden et al., 2018;
98 Hedrick et al., 2019). Caliper-based linear morphometrics have been previously used to assess
99 interspecific variability in *Artibeus* (Lim, 1997; Guerrero et al., 2003; Lim et al., 2008; Balseiro
100 et al., 2009; Larsen et al., 2010; Marchán-Rivadeneira et al., 2010), and these studies largely
101 found that there was low interspecific variation across members of the genus. However,
102 geometric morphometrics has been shown to be able to distinguish shape trends more effectively
103 than linear morphometrics (Mutanen and Pretorius, 2007; Zelditch et al., 2012; Schmieder et al.,
104 2015). Thus the relatively small differences in skull shape and size among *Artibeus* species will
105 potentially be easier to capture and distinguish using geometric morphometrics in comparison

106   with linear morphometrics as it captures shape more holistically and allows for better separation
107   of size and shape. This could potentially uncover previously unknown morphological size and
108   shape partitioning in the *Artibeus* species complex. However, geometric morphometric analyses
109   have yet to be used to analyze variation in *Artibeus*.
110   The overarching goal of this study is to expand upon previous studies by employing
111   geometric morphometrics on a sample of 279 crania for eleven species of the *Artibeus* species
112   complex (22 species total) to address the following questions: (1) Do different members of the
113   *Artibeus* species complex differ in size and shape? Significant differences between species may
114   suggest differences in niche partitioning via morphological innovation or conversely suggest
115   non-adaptive processes such as genetic drift or non-morphological adaptive bases for niche
116   partitioning (e.g., echolocation differences, biting behavior). (2) How have factors such as
117   phylogeny, sexual dimorphism, and geography structured that variation? Interspecific analyses
118   are done to evaluate differences in size, shape, and sexual dimorphism across the *Artibeus*
119   species complex. Based on previous studies (Marchán-Rivadeneira et al., 2010), I predict that the
120   *Artibeus* species complex will separate into two clear size groups (small and large *Artibeus*) and
121   that there will be additional separation within those two groups by size. Similarly, I predict that
122   shape will not differ substantially across species following previous studies based on linear
123   morphometrics (Balseiro et al., 2009; Marchán-Rivadeneira et al., 2010). I predict significant
124   sexual dimorphism based on previous studies that have found male and female *Artibeus* species
125   to exhibit differing foraging behaviors (Kunz & Diaz, 1995). To assess intraspecific variation
126   and geographical variation in the *Artibeus* species complex, *A. lituratus* is heavily sampled
127   across its range. I hypothesize that there is shape and size variation across *A. lituratus*' range
128   based on previous studies finding correlations between *A. lituratus* skull shape and
129   environmental variables (Marchán-Rivadeneira et al., 2012). Using these data, I address the
130   degree of morphological variation in the *Artibeus* species complex, discuss the underlying causes
131   for that variation, and shed light on the radiation of the *Artibeus* complex.
132
133   **Materials & Methods**
134   *(a) Materials and Initial Analyses*
135   *Artibeus* spp. (n = 279) crania were photographed in lateral and ventral view at the
136   Louisiana State University Museum of Natural Sciences (LSUMZ) using a Canon EOS 70D
137   fitted with a Canon EF-S 60 mm f/2.8 Macro USM fixed lens mounted on a photostand to ensure
138   the same angle was used in each picture. Two separate datasets were used, one to analyze
139   interspecific variation (n = 186) and one to analyze intraspecific variation in *A. lituratus* (n =
140   113). The interspecific sample included *A. anderseni* (n = 8), *A. phaeotis* (n = 20), *A. cinereus* (n
141   = 20), *A. toltecus* (n = 14), *A. aztecus* (n = 9), *A. fraterculus* (n = 20), *A. obscurus* (n = 20), *A.
142   jamaicensis* (n = 20), *A. planirostris* (n = 20), *A. lituratus* (n = 20), and *A. fimbriatus* (n = 15)
143   (Fig. 1). Classifications were done according to Rojas et al. (2016) who considered all of these
144   species to belong to *Artibeus,* but note that *A. anderseni, A. aztecus, A. cinereus, A. phaeotis,* and
145   *A. toltecus* are also sometimes classified as *Dermanura*. To reduce confusion, the term '*Artibeus*
146   species complex' is used in this study to refer to all species included in this study.
147   The intraspecific sample included populations of *A. lituratus* from Argentina (n = 20),
148   Belize (n = 6), Costa Rica (n = 11), Paraguay (n = 20), Peru (n = 20), Trinidad (n = 7), and two
149   localities in Mexico (Colima, n = 8; Tabasco, n = 21). Each population here is named based on
150   the country of origin. 'Countries' were used as proxies for populations due to limited specimen
151   availability at individual localities in the visited museum collections. Generally, all specimens

152 from each 'country' are quite close to one another geographically. Two populations were
153 sampled in Mexico, which are ~1500km apart and are thus referred by the Mexican state where
154 they were collected. Full details regarding collection information are present in the supplemental
155 information. *A. lituratus* was selected for analyzing intraspecific variation in *Artibeus* based on
156 its large range and its abundance and availability in the LSUMZ collections. I aimed to include
157 20 specimens for each species and country respectively, but that was not always possible due to
158 limitations in the museum collections. All specimens were coded for sex and I aimed to have
159 equal numbers of males and females in each sample (53 males, 60 females; see Supplemental
160 Information). To keep sample sizes balanced in the interspecific analyses, the Argentina *A.*
161 *lituratus* specimens (n = 20) were included in the interspecific dataset. *A. lituratus* specimens
162 from other localities were only examined in the intraspecific dataset.
163   Skulls were landmarked and semi-landmarked in tpsDIG2 (Rohlf, 2006) in lateral and
164 ventral views. Landmarks represent homologous anatomical loci while semi-landmarks represent
165 homologous curves. Eleven landmarks and one semi-landmark curve consisting of 15 semi-
166 landmarks were digitized in lateral view and seventeen landmarks and one semi-landmark curve
167 consisting of 10 semi-landmarks were digitized in ventral view (Fig. 2, Table S1). Landmarks
168 were imported into RStudio v. 1.1.463 (R Core Development Team, 2019) and opened in
169 *geomorph* v. 3.0.7 (Adams & Otárola-Castillo, 2013). Landmarks were subjected to Generalized
170 Procrustes Analysis (GPA) and semi-landmarks were evenly spaced and were slid according to
171 the bending energy criterion (Bookstein, 1997; Perez et al., 2006; Zelditch et al., 2012). This
172 generated two centroid sizes per specimen (one lateral view and one ventral view). Each centroid
173 size was used in analyses with its corresponding shape data (e.g., lateral view centroid size
174 analyzed with lateral view shape data). An error analysis was performed whereby one individual
175 (LSUMZ 9425) was landmarked 10 additional times in both lateral and ventral views to assess
176 within individual landmarking error. All replicates of this specimen were then plotted in
177 principal component morphospace to evaluate general shape trends and ensure that the replicates
178 of the same individual clustered together closely with other replicates (Fig. S1), prior to running
179 analyses on the dataset as a whole.
180
181 *(b) Interspecific Data Analyses*
182   To analyze trends in the data, both lateral and ventral landmark configurations were
183 subjected to principal component analysis (PCA). Principal components (PCs) that represented
184 greater than 10% of total shape variation were examined. To address whether shape varied by
185 size for both the lateral and ventral datasets, relationships between the common allometric
186 component (CAC) of shape variation (Mitteroecker et al., 2004) were tested against log10-
187 transformed centroid size using a Procrustes ANOVA that was permuted 999 times. The CAC
188 represents the allometric trend in the data. These data were represented graphically both as
189 regressions and using violin plots of log10-transformed centroid size. Additionally, Procrustes
190 ANOVAs were done to analyze the relationship between shape, species, sex, and size (shape ~
191 species * sex * size) in both views where size was represented by log10-transformed centroid
192 size. Finally, sexual size dimorphism was analyzed in both views (size ~ species * sex). Due to
193 sample size limitations, sexual dimorphism was examined in the *Artibeus* species complex as a
194 whole, and in *A. lituratus*, which was sampled at a higher rate for the intraspecific analyses (see
195 below).
196   Species means of shape for lateral and ventral views were then taken for all 11 species to
197 quantify the degree of phylogenetic signal in the data. Species means were first subjected to GPA.

198 Shape data and log10-transformed centroid sizes were evaluated for phylogenetic signal using
199 Blomberg's K statistic modified for multivariate shape data (Kmult) (Blomberg et al., 2003;
200 Adams, 2014) in *geomorph*. This was done using the phylogeny from Rojas et al. (2016). In
201 addition to the Procrustes ANOVAs discussed above, phylogenetically-corrected Procrustes
202 ANOVAs were performed on means data. This required combining each species into a single
203 mean (thereby losing the sex component). The species phylogeny was plotted onto a PCA of
204 mean shapes to visually examine how phylogeny and morphology related to one another in
205 morphospace. To better understand the evolutionary processes that underlie phylogenetic signal
206 in the data, patterns of disparity accumulation through time were calculated using the dtt function
207 in *geiger* (Harmon et al., 2008). By analyzing disparity through time, it is possible to better
208 understand whether shape evolved under a Brownian motion pattern or through punctuated
209 bursts of disparity.
210   In order to further analyze differences between species, the *nicheROVER* package
211 (Swanson et al., 2015) was utilized. This analysis was developed to evaluate niche overlap with
212 multidimensional data and has been previously applied to shape data (Machado et al., 2018).
213 Separate analyses were run for the lateral and ventral datasets utilizing principal components 1
214 and 2 and log10-transformed centroid size to quantitatively assess how much overlap is present
215 in shape and size between species pairs. Posterior distributions were generated for these values
216 for each species using 10,000 permutations. The overlap function was then used to calculate
217 overlap metric estimates at a 95% confidence interval. Finally, the posterior probabilities that a
218 given species overlaps with another species in size and shape were plotted.
219
220 *(c) Intraspecific Data Analyses*
221   Lateral and ventral *A. lituratus* crania were subjected to PCA as was done in the
222 interspecific analyses. Procrustes ANOVAs were performed to assess the relationship between
223 shape, sex, size, and country (shape ~ sex + size + country) in both views, with size represented
224 by log10-transformed centroid size. Posthoc tests were performed using the advanced.procD.lm
225 function in *geomorph* to generate pairwise comparisons (Collyer et al., 2015). Sexual size
226 dimorphism was assessed in base R (size ~ country + sex) for both views.
227   To visualize how close individuals in portions of the geographic range (countries) cluster
228 to one another, distance matrices based on Euclidean distances were calculated for country
229 means in base R using all principal components for both lateral and ventral datasets (R Core
230 Development Team, 2019). Hierarchical clustering was then performed using unweighted pair-
231 group method with arithmetic means (UPGMA) through the hclust function. These clusters were
232 then plotted as dendrograms. To determine how well the dendrograms reflect the underlying
233 hierarchical structure, the cophenetic correlation coefficient was calculated (Sneath & Sokal,
234 1973). This compares heights of tips above the node that they are joined to with the observed
235 correlation matrix (Zelditch et al., 2012).
236
237 **Results**
238 *(a) Interspecific Results:*
239   In principal component space, large *Artibeus* and small *Artibeus* groups separated in the
240 lateral and ventral datasets along PC1 (Fig. 3, Fig. S2 for colorblind version). The separation is
241 less clear in the lateral dataset than the ventral dataset (see Table S2 for full results).
242   In the lateral PCA, PC1 accounted for 54.5% of total variation. The small *Artibeus* (*A.*
243 *anderseni, A. phaeotis, A. cinereus*, and *A. toltecus*, and *A. aztecus*) plotted on the negative PC1 axis

244   while the large *Artibeus* (*A. fraterculus, A. obscurus, A. jamaicensis, A. planirostris, A. lituratus*,
245   and *A. fimbriatus*) plotted on the positive PC1 axis. While PC1 was largely structured by size,
246   some of the largest (e.g., *A. lituratus*) and smallest (e.g., *A. cinereus*) species plotted towards the
247   center of morphospace rather than on the ends defined by PC1. Therefore, PC1 incorporated both
248   size and shape data. Taxa on the negative end of PC1 tended to have a shorter rostrum than those
249   on the positive end of PC1 (Fig. 3A). PC2 accounted for 17.5% of total variation and separated
250   out species within larger clusters. Specimens on the positive end of PC2 had a less pronounced
251   dome shape to their crania than those on the negative end of PC2. Specimens on the negative end
252   of PC2 also had a more caudally positioned zygomatic arch relative to the position of the
253   external acoustic meatus. Within the small *Artibeus* cluster, *A. phaeotis*, *A. toltecus*, and *A.*
254   *anderseni* plotted on the negative PC2 axis while *A. aztecus* and *A. cinereus* plotted on the
255   positive PC2 axis. *A. cinereus* overlapped strongly with *A. jamaicensis* and *A. fraterculus*. In the
256   large *Artibeus* cluster, all taxa plotted in one large poorly differentiated group. However, *A.*
257   *fimbriatus* and *A. planirostris* tended to have higher PC1 scores than the other large *Artibeus*
258   species. Additional PCs accounted for less than 10% of total variance.
259   Shape and log-transformed centroid size were significantly correlated for the lateral
260   dataset (p < 0.001, R^2 = 0.369). The small *Artibeus* group and large *Artibeus* group separated in
261   centroid size and shape (Fig. 4A). All small *Artibeus* species occupy different sizes with minimal
262   overlap (Fig. 4B). *A. cinereus* and *A. toltecus* overlap along the common allometric component
263   of shape, but have different size ranges (*A. cinereus* mean CS = 3.57, *A. toltecus* mean CS =
264   3.81). *A. aztecus* and *A. phaeotis* show a similar situation where they overlap in shape, but not in
265   size (Fig. 4A, B). *A. anderseni* is the smallest taxon included (mean CS = 3.28). There are two
266   size groups for the large *Artibeus* taxa, one including *A. fraterculus, A. obscurus*, and *A.*
267   *jamaicensis* and the other including *A. lituratus, A. planirostris*, and *A. fimbriatus* (Fig. 4B).
268   Within the smaller large *Artibeus* cluster, *A. fraterculus* and *A. jamaicensis* overlap in shape, but
269   *A. obscurus* does not. In the larger large *Artibeus* cluster, *A. planirostris* and *A. fimbriatus*
270   overlap in shape, but *A. lituratus* does not.
271   Similar to the lateral PCA, in the ventral dataset large and small *Artibeus* are separated
272   with small *Artibeus* plotting on the negative end of PC1 and large *Artibeus* plotting on the
273   positive end of PC1 (Fig. 3B). Unlike the lateral PCA, the two clusters do not have any overlap.
274   PC1 accounted for 51.7% of the total variance and PC2 accounted for 11.4% of total variance.
275   Additional PCs accounted for less than 10% of the total variance. Taxa on the negative end of
276   PC1 had a relatively shorter rostrum and longer basicranium than those on the positive end of
277   PC1. Along PC1, the large *Artibeus* cluster had a clear separation between an overlapping group
278   composed of *A. lituratus*, *A. jamaicensis*, *A. fraterculus*, and *A. obscurus* and a group composed
279   of *A. fimbriatus* and *A. planirostris*. *A. fimbriatus* and *A. planirostris* were further separated
280   along PC2. Within the small *Artibeus* group, PC2 separated *A. cinereus* from the other small
281   *Artibeus* taxa (*A. phaeotis*, *A. aztecus*, *A. toltecus*, and *A. anderseni*), which overlapped.
282   Specimens on the negative end of PC2 had a wider skull with a more curved zygomatic arch than
283   those on the positive end of PC2.
284   Size and shape were similarly correlated in the ventral dataset (p < 0.001; R^2 = 0.461).
285   Compared to the lateral dataset, the taxa had less spread along the common allometric coefficient
286   shape axis (Fig. 4C). The log-transformed centroid size spread for the lateral dataset and the
287   ventral dataset strongly agreed (Figs. 4B, D). As in the lateral dataset, the small and large
288   *Artibeus* groups were strongly separated in centroid size. *A. anderseni* differed in size and shape
289   from other small *Artibeus* taxa. However, *A. phaeotis, A. cinereus, A. toltecus,* and *A. aztecus* all

290   overlapped on the shape axis. The large *Artibeus* taxa split into two size-based groups as in the
291   lateral dataset. Unlike the lateral dataset, *A. fraterculus, A. obscurus*, and *A. jamaicensis*
292   overlapped on the shape axis. Similar to the lateral dataset, *A. planirostris, A. lituratus*, and *A.*
293   *fimbriatus* form a cluster. *A. planirostris* and *A. fimbriatus* have similar sizes and shapes whereas
294   *A. lituratus* has a different shape from the other two taxa.
295   NicheROVER analyses similarly demonstrated minimal overlap between species when
296   size and shape (PC1, 2) axes were considered (Fig. S3, S4). In lateral view, only *A. jamaicensis*
297   and *A. fraterculus* and *A. lituratus, A. fimbriatus*, and *A. planirostris* had more than 50% mean
298   overlap. In ventral view, *A. jamaicensis, A. fimbriatus*, and *A. obscurus* had over 50% mean
299   overlap, but other species did not.
300   Based on the Procrustes ANOVA of the lateral shape dataset (Tables 1, S3), all main
301   factors (species, sex, and size) were significant (p < 0.001). Further, the interaction of species
302   and sex was also significant (p < 0.001) showing that different sexes are different shapes for
303   different species (intraspecific sexual shape dimorphism). The interaction of species and size was
304   also significant (p < 0.001). Shape and the interaction of sex and size was not significant (p =
305   0.919). Finally, the interaction of species, sex, and size was significant with respect to shape (p <
306   0.001) showing that allometric relations change with species and with each sex in each species.
307   The trends for the ventral dataset (Table 2) were the same except that the interaction of sex and
308   size was significant (p = 0.003).
309   In lateral view, both shape (K_{mult} = 0.80, p = 0.008) and size (K_{mult} = 2.51, p < 0.001)
310   were significantly correlated with phylogeny. Similarly, the ventral dataset showed that both
311   shape (K_{mult} = 1.04, p = 0.007) and size (K_{mult} = 2.50, p < 0.001) were significantly correlated
312   with phylogeny (see Table S4 for PCA results). Mapping the phylogeny on the species means in
313   principal component space demonstrates a separation between small and large *Artibeus* in
314   morphospace with less clear trends within each group (Fig. S5A, S5B). In lateral view, there is a
315   peak in disparity at approximately 5 mya, which is at the timing of the split between small and
316   large *Artibeus* (Fig. S5C). This suggests a burst in morphological disparity at that time. Disparity
317   accumulation in ventral view generally follows Brownian motion with a small increase in
318   disparity at 5 mya (Fig. S5D). Using phylogenetically corrected Procrustes ANOVAs, neither
319   size nor species were significantly correlated with lateral or ventral shape (Table S4). This is
320   likely due to the strong separation in both size and shape between the small *Artibeus* and large
321   *Artibeus*, which each form a monophyletic group. Given a large amount of individual variation
322   and species overlap, the mean shapes are likely simplifying the trends and reducing the signal.
323   Therefore, the discussion will largely concern the non-phylogenetically corrected results
324   recognizing that there is a phylogenetic component to cranial shape in the *Artibeus* species
325   complex.
326
327   *(b) Intraspecific Results:*
328   Although there was a substantial amount of overlap in principal component space, *A.*
329   *lituratus* specimens grouped by locality (country) in both the lateral and ventral datasets,
330   demonstrating some intraspecific geographic variation within *A. lituratus* (Fig. 5; see Table S5
331   for full results).
332   In the lateral dataset, PC1 accounted for 31.7% of the total variation and PC2 accounted
333   for 24.1% of the total variation (Fig. 6A). Specimens on the positive PC1 axis had relatively
334   longer zygomatic arches and a somewhat more compact skull. Specimens from Argentina
335   exemplified this morphotype. Specimens on the negative end of PC1 had shorter zygomatic

336   arches with a less compact skull, shown by specimens from Trinidad. While these specimens
337   group by country in morphospace, it should be noted that the shape differences are quite minor.
338   In the ventral dataset, PC1 accounted for 25.9% of total variation while PC2 accounted for
339   13.4% of total variation (Fig. 6C). Specimens on the positive PC1 axis had somewhat more
340   compact skulls with flatter zygomatic aches, exemplified by specimens from Argentina and
341   Paraguay, than taxa at the negative end of PC1. However, as with the lateral dataset, these shape
342   differences were quite minor in spite of clear country-based groupings in morphospace.
343   Based on a Procrustes ANOVA (lateral shape ~ sex + size + country), lateral shape was
344   significantly correlated with sex ($p = 0.002$), size ($p < 0.001$), and country ($p < 0.001$).
345   Additional pairwise tests were performed to establish significances between countries using the
346   advanced.procD.lm function in *geomorph* (See Table 3, above diagonal for lateral view; for Z-
347   scores, see Table S6). Cranial centroid size in lateral view was lower in the northern localities
348   (Belize, Mexico, Costa Rica) in comparison with the southern ones (Peru, Trinidad, Paraguay,
349   Argentina) (Table 4). The ventral shape dataset was significantly corelated with size ($p < 0.001$)
350   and country ($p < 0.001$), but not sex ($p = 0.39$) under the Procrustes ANOVA model (ventral
351   shape ~ sex + size + country). Pairwise comparisons showed fewer significant differences in the
352   ventral dataset in comparison with the lateral dataset (Table 3, below diagonal for ventral view;
353   for Z-scores, see Table S6). Size was significantly correlated with country in both lateral ($p <$
354   0.001) and ventral ($p < 0.001$) views. Sex was correlated with size in lateral view ($p = 0.027$), but
355   was marginally significant in ventral view ($p = 0.063$). The average centroid size in ventral view
356   strongly correlated with the average centroid size in lateral view such that the more northern
357   countries had smaller average centroid sizes than the more southern countries (Table 4).
358   The UPGMA analyses had cophenetic coefficients that suggest that the dendrograms do
359   display underlying hierarchy (lateral dataset cophenetic coefficient = 0.85; ventral dataset
360   cophenetic coefficient = 0.83). In both datasets, the Mexican localities, Costa Rica, and Trinidad
361   formed a cluster (Figs. 6B; 6D). This did not include Belize in either case. In the lateral dataset,
362   Belize and Peru grouped together and Argentina and Paraguay grouped together. In ventral view,
363   Belize and Paraguay grouped together and Argentina and Peru grouped together.
364
365   **Discussion**
366   Speciation can occur through numerous avenues, including vicariance or via
367   modifications in resource use of species in sympatry. Quantifying morphological variation can
368   grant insight into how species may be converging on similar morphologies or diverging into
369   disparate morphologies, whether that is occurring interspecifically or intraspecifically across a
370   wide geographical range. As a result, such analyses help to shed light onto the underlying
371   mechanisms structuring the degree of morphological variation in a group. Bats are one of the
372   most diverse mammalian groups, with numerous species living in sympatry with closely related
373   species. The phyllostomids are one of the most diverse bat families (Shi & Rabosky, 2015) and
374   the *Artibeus* species complex is highly diverse within the Phyllostomidae, making them an
375   excellent group with which to ask questions about interspecific and intraspecific morphological
376   variation. The present study demonstrates that species within the *Artibeus* species complex have
377   diverged into discordant morphologies and/or sizes, potentially allowing them to occupy
378   different niches. Further, significant intraspecific differences were found within *A. lituratus*
379   across its range, demonstrating that within species variation is an important factor to consider
380   when analyzing skull shape in bats. However, no clear patterns of geographical variation were
381   found.

382
383 *Interspecific Variation of the Artibeus Species Complex*
384   This study demonstrated clear species level differences in cranial size and shape across
385 the *Artibeus* species complex (Tables 1; 2), which may suggest niche partitioning of species if
386 these differences impact biting performance or resource use. The present study confirmed the
387 broad size difference between small and large *Artibeus* found in prior studies that used linear
388 morphometrics (Lim, 1997; Ortega & Castro-Arellano, 2001; Larsen et al., 2010; Marchán-
389 Rivadeneira et al., 2010). Principal component 1 in lateral and ventral views were largely related
390 to size and showed clear separation between these two groups (Fig. 3). This result was
391 corroborated by an allometric analysis demonstrating a significant relationship between size and
392 shape with small *Artibeus* species separating fully from large *Artibeus* species in both lateral (Fig.
393 4A) and ventral (Fig. 4C) views. It was further shown by a lack of overlap in size and shape
394 variables (Fig. S3, S4).
395   In addition to the division between the broader small and large *Artibeus* groups, the
396 present analysis found fine-scale size and shape-based divisions within each group. While some
397 previous studies have found species level differences in cranial shape variation in the *Artibeus*
398 species complex (Lim et al., 2008), the majority of previous studies have found that cranial shape
399 does not substantially vary within either large or small *Artibeus* groups (e.g., Balseiro et al.,
400 2009; Marchán-Rivadeneira et al., 2010). Two clear size-based groups were found in the large
401 *Artibeus*, which are present in both lateral view (Fig. 4B) and ventral view (Fig. 4D). The first
402 group included *A. fraterculus*, *A. obscurus*, and *A. jamaicensis* and the second included *A.*
403 *planirostris*, *A. lituratus*, and *A. fimbriatus*. This is in agreement with Ortega and Castro-
404 Arellano (2001), who noted that *A. planirostris* and *A. fraterculus* differed in size. Variation in
405 shape across these species was also present, with *A. obscurus* having a different shape from *A.*
406 *fraterculus* and *A. jamaicensis* in the first group and *A. lituratus* having a different shape than *A.*
407 *planirostris* and *A. fimbriatus* in the second group (Fig. 4A, C). Additionally, the small *Artibeus*
408 had clear size separation across all species examined (*A. anderseni*, *A. phaeotis*, *A. cinereus*, *A.*
409 *toltecus*, and *A. aztecus*). Just like with the large *Artibeus*, the small *Artibeus* differed in shape as
410 well, with *A. cinereus* and *A. toltecus* having similar shapes, which were different from *A.*
411 *phaeotis* and *A. aztecus*, especially in lateral view (Fig. 4A). *A. anderseni* had a different shape
412 from all small *Artibeus* species. Overall, the majority of species differed from one another in
413 cranial size, shape, or a combination of the two (Fig. S3; S4).
414   Phylogeny was significantly correlated with skull shape in both the lateral and ventral
415 datasets. Phylogenetic comparative methods using species means showed a lack of significance
416 between shape, size, and species (Table S4), which may suggest that some of the shape
417 differences across species uncovered in the non-phylogenetically corrected ANOVAs may be
418 related to allometric differences or drift rather than morphological changes related to skull
419 function. This lack of significance may also be related to the strong divide in both shape and size
420 between large and small *Artibeus*. Examining shape data of species means in a
421 phylomorphospace revealed strong clustering of small *Artibeus* and large *Artibeus* species, but
422 less phylogenetic influence within each broader group (Fig. S5A, B). Evaluating disparity
423 through time demonstrated a spike in disparity at the time when the small and large *Artibeus* split
424 (Fig. S5C, D). This supports the idea that the main phylogenetic influence in the data was the
425 division between small and large *Artibeus*, which are sometimes considered separate genera
426 (Redondo et al., 2008).

427   Behavioral plasticity in feeding habits can drive variation both within species and
428   between species. Dumont and O'Neal (2004) found that different pteropodid species perform
429   different biting behaviors when eating fruits of different hardnesses and suggested that some
430   species access hard fruit diets by changing behavior while others may do so through
431   morphological changes. Recently, Hedrick et al. (2020) showed that it is likely behavioral
432   plasticity rather than morphological shape change of their proximal limb bones that has allowed
433   diversification of rodents into varied locomotor niches, suggesting that behavioral plasticity
434   rather than morphological change can facilitate diversification. Therefore, it is likely that
435   morphological variation is not the only factor that has allowed the *Artibeus* species complex to
436   proliferate, and that behavioral plasticity may be another factor. Although figs make up 78% of
437   the diet of *Artibeus jamaicensis* (Ortega & Castro-Arellano, 2001) and *Artibeus* spp. has been
438   considered a specialist on Cecropiaceae and Moraceae (Fleming, 1986), fig trees are not
439   available as a food resource at all times of the year (August, 1981). For example, *A. jamaicensis*
440   and *A. lituratus* have been shown to be folivorous for part of the year (Zortéa & Mendes, 1993;
441   Kunz & Diaz, 1995) and *A. lituratus* is known to have a more generalist diet in regions where
442   figs are not as abundant (Galetti & Morellato, 1994). Given annual dietary variation, a
443   combination of morphological and behavioral plasticity may have led *Artibeus* spp. to have a
444   previously unrecognized amount of both interspecific and intraspecific variation. Small *Artibeus*
445   species tend to have a taller, more dome shaped skull with a shorter rostrum, indicating a higher
446   mechanical advantage than the less tall, rostrocaudally long skulls of large *Artibeus* species (Fig.
447   3). Since the small *Artibeus* species have smaller skulls compared to the large *Artibeus*, they may
448   compensate for their small skull size by enhancing their mechanical advantage to consume hard
449   figs that the large *Artibeus* species are able to eat as a result of their larger skull size.
450   Alternatively, morphological variation in *Artibeus* spp. may be related to allometry or drift rather
451   than function. Future work evaluating skull shape variation in *Artibeus* spp. across its
452   geographical range in connection with field studies demonstrating which fruits are eaten at each
453   locality will help to establish a form-function relationship. Such work will also uncover the role
454   of behavioral and dietary plasticity in *Artibeus* spp. to allow a better understanding of how these
455   factors and the morphological diversity demonstrated in the present study may have shaped the
456   evolution of the *Artibeus* species complex.
457
458   *Sexual Dimorphism*
459   In addition to interspecific morphological variation, this study showed that both sexual
460   size dimorphism and sexual shape dimorphism were present in lateral and ventral views in the
461   *Artibeus* species complex as a whole. *A. lituratus* had significant sexual shape and size
462   dimorphism in lateral view, but not in ventral view. In lateral view, the females had a lower skull
463   profile than males (Fig. 7A). Further, *A. lituratus* females were larger than males (Fig. 7C, D).
464   Female *A. obscurus* have also been noted to be larger than males (Brosset & Charles-Dominique,
465   1990; Eisenberg & Redford, 1989; Simmons & Voss, 1998). As sexual size dimorphism is
466   present in lateral view for *A. lituratus* and is only marginally significant in ventral view (Table
467   S6), even though the two size metrics strongly agree, the two-dimensional view used to calculate
468   centroid size may have a bearing on significance. Further, since sexual dimorphism was assessed
469   in the interspecific data at the genus level as a result of sample size limitations, it is not possible
470   to determine which specific *Artibeus* species were sexually dimorphic (with the exception of *A.*
471   *lituratus*). Given the low R^2 value associated with sex in the interspecific data, it is likely that
472   some species display sexual dimorphism while others do not. A deeper analysis of other *Artibeus*

473   species with large sample sizes, similar to the one performed here for *A. lituratus* will help
474   clarify sexual dimorphic trends for other *Artibeus* species.
475   The significant sexual dimorphism found here has implications for behavioral ecology
476   and niche partitioning in the *Artibeus* species complex. Behavioral differences between sexes
477   have been noted in *A. jamaicensis (*Kunz & Diaz, 1995). Males forage primarily near their roosts,
478   allowing them greater time for roost defense, while females forage greater distances and for
479   longer periods of time (Morrison, 1979; Morrison & Morrison, 1981). These differing strategies
480   may affect cranial morphology. For example, females have the opportunity to seek out higher
481   quality food since they do not have to rely on the food near their roosts. Thus different feeding
482   behaviors in each sex might have an impact on sexual size dimorphism in cases where males and
483   females are feeding on different quality fruits. For example, body mass has been correlated with
484   fruit size in *A. jamaicensis* and *A. lituratus* (Ortega & Castro-Arellano, 2001). Since fruit
485   hardness and skull shape have also been correlated in a wide variety of phyllostomids (Freeman,
486   2000; Nogueira et al., 2009; Dumont et al., 2012; Hedrick & Dumont, 2018), these differences
487   may also lead to the sexual shape dimorphism found in the present study's data if males and
488   females choose fruits of different hardnesses. In lateral view, male *A. lituratus* have a slightly
489   taller, more dome-shaped skull with a more pronounced sagittal crest and shorter rostrum (Fig.
490   7A), which suggests that they are able to consume somewhat harder fruit given a somewhat
491   higher mechanical advantage for the temporalis muscle. The shape of the zygomatic arch in
492   ventral view is identical in male and female *A. lituratus* indicating no difference in their masseter
493   muscle (Fig. 7B). The presence of a stronger sagittal crest on male skulls leads to the potential
494   hypothesis that male *A. lituratus* are capable of higher bite forces and eating harder fruits than
495   females (Santana et al., 2010), although this needs to be thoroughly evaluated using bite force
496   data. Other alternative hypotheses related to higher sagittal crests in males may include biting
497   during male-male combat or tent-making. Alternative to the functional-related hypothesis that is
498   proposed, sexual selection for larger size in females may play a role in skull shape. Female *A.*
499   *lituratus* have larger skulls than males (Fig. 7C, D), which is common among bat species where
500   the female is typically larger so she can maintain homeothermy during pregnancy and fly while
501   carrying her pups while they are nursing (Williams and Findley, 1979). Larger size in females
502   may lead to a less developed sagittal crest in comparison with males as they may be able to eat
503   relatively harder foods by virtue of larger body size. More work on potential dietary differences
504   between male and female *Artibeus* species will need to be done in order to better elucidate these
505   results.
506
507   *Intraspecific and Geographical Variation in Artibeus lituratus*
508   *Artibeus lituratus* has an expansive range from Mexico to Argentina. This study
509   demonstrates substantial geographical variation in *A. lituratus* skull size and shape with
510   specimens forming country locality clusters in morphospace (Fig. 6A, C). However, the data do
511   not have an obvious pattern of clinal variation, which is demonstrated most clearly by the
512   UPGMA results. In lateral view, two main groups formed using UPGMA of shape data, one
513   containing Peru and Belize, and the other with Paraguay, Argentina, Trinidad, Costa Rica, and
514   the two Mexican localities. The ventral view data had a similar core with the two Mexican
515   localities, Costa Rica, and Trinidad grouping together, but the other country groupings changed
516   (Fig. 6B, D). Belize being outside of the core group of northern countries in spite of being one of
517   the northernmost localities sampled highlights the lack of clinal structure in the shape data. The
518   pairwise results also demonstrate some lack of consensus between the lateral and ventral views

519   for many countries. For example, Belize is significantly different from all countries other than
520   Costa Rica, Trinidad, and Paraguay in lateral view, but is significantly different from all
521   countries other than Costa Rica and the two Mexican localities in ventral view. In this example,
522   the ventral view suggests a geographical cluster of northern localities, while the lateral view
523   suggests no geographical clustering. Size variation in *A. lituratus* appears to generate two groups,
524   north and south. Specimens from Belize, Mexico, and Costa Rica had the smallest average
525   centroid sizes among specimens sampled while specimens from Argentina, Trinidad, Peru, and
526   Paraguay had the largest (Table 4). General clinal size variation has been reported in other bats
527   as well (Nargosen & Tamsitt, 1981; Owen et al., 1984; Storz et al., 2001) and a wide variety of
528   other species (birds, James, 1970; mammals, Koch, 1986; insects, Chown and Gaston, 2010). In
529   spite of this overall grouping, there was no clear clinal pattern within either the northern or
530   southern groups.
531   Only in the extreme northern and southern localities did a consistent shape pattern
532   emerge. In lateral view, Argentina is significantly different from all other localities, and in
533   ventral view it is significantly different from all northern localities (Mexico, Belize, Costa Rica),
534   while not significantly different from South American localities (Paraguay, Peru, Trinidad).
535   Similarly, the two Mexican localities are significantly different from all localities other than
536   Costa Rica in lateral view while they are significantly different from all South American
537   localities in ventral view and not different from the other northern localities. This strongly
538   suggests that the *A. lituratus* range only has substantial differences at northern and southern
539   extremes and otherwise does not exhibit a clinally graded morphological spectrum for cranial
540   shape. This demonstrates that analyzing specimens from across a species' range will grant a
541   better understanding of the shape disparity within that taxon, especially in taxa with large ranges
542   such as *A. lituratus* where significantly different morphologies at the extremes of the species'
543   range may be missed.
544   The lack of an obvious geographical pattern in these data may be due to differences in
545   environmental conditions at the localities where the bats were collected rather than spatial
546   differences. The present study did not assess environmental variables, but instead looked for
547   general skull shape and size differences in relation to geographical distance. In *Eptesicus fuscus*,
548   Burnett (1983) found that both climatic factors and geography affected morphology, with
549   geography tending to be a better predictor for wing shape and environment tending to be a better
550   predictor for skull shape. Using linear morphometrics, Marchán-Rivadeneira et al. (2012) found
551   that skull size variation in *A. lituratus* was tied closely to environmental variables. Factors such
552   as seasonality and precipitation were tightly correlated with skull size. Stevens et al. (2016)
553   examined wing shape variation in *A. lituratus* in the Atlantic forests of Paraguay and Argentina
554   and found that environmental variables accounted for 75% of variation across sites. They suggest
555   that this is due to local adaptations in wing morphology, which enhance maneuverability in some
556   environments. Therefore, there may be a larger pattern among bats that both wing shape and
557   cranial shape are more closely tied to environmental factors than geographical distances. Further,
558   taxa in the Amazon are often considered to present more of a mosaic of characters rather than a
559   clear pattern, such as clinal variation (Bates et al., 1998; Ferreira et al., 2014). This may be the
560   case for *A. lituratus* crania.
561   Genetic differences across the wide *A. lituratus* range may also have led to the north-
562   south size differences that are captured in this study. Two subspecies are sometimes recognized
563   (*A. lituratus intermedius* and *A. lituratus palmarus*), though are also often considered different at
564   the specific level (*A. lituratus* and *A. intermedius*) (Simmons, 2005; Redondo et al., 2008).

565 Unfortunately, the subspecies identification was not available for the specimens included in this
566 analysis so this could not be assessed. Regardless of subspecies identification, genetic drift may
567 be a factor generating the difference in size between northern and southern specimens of *A.*
568 *lituratus* as well. Given this study's clear documentation of the range of individual variation
569 present in *A. lituratus*, a more specific study examining skull shape and size in habitats with
570 different environmental variables in the northern and southern parts of the *A. lituratus* range
571 would allow for more concrete conclusions.
572
573 **Conclusions**
574   The *Artibeus* species complex is a widespread, highly diverse lineage, with many species
575 that live in sympatry. Being able to quantify variation and differentiate species morphologically
576 is a step towards understanding the diversification of the *Artibeus* species complex and the
577 factors that drove its radiation more generally. Morphological variation was not only evident
578 both between the small *Artibeus* and large *Artibeus* groups, but fine-scale size and shape
579 variation was also evident within both groups. Shape data were significantly correlated with
580 phylogeny, likely due to the strong clustering of species within the small and large *Artibeus*
581 groups. Further, given that *Artibeus* feed on different fruits throughout the year, it is possible that
582 a combination of morphological and behavioral plasticity has led to the modern diversity of the
583 group. This study demonstrated morphological separation between males and females, perhaps
584 due to these behavioral drivers; however, sex accounted for a small percent of total shape
585 variation. Finally, geographical variation is a clear factor governing intraspecific variation in *A.*
586 *lituratus*. This variation is not obviously driven by clinal factors and likely relates to site-level
587 environmental variables or drift rather than broad geographical distances. Being able to
588 accurately delineate and discriminate among species is critical for both taxonomy and for
589 conservation initiatives (Fernandez et al., 2009) and quantifying inter- and intraspecific variation
590 across a broad geographic range grants insight into how morphological variation in a group is
591 structured, allowing for second-order analyses. Future work on the ecological and behavioral
592 variables that have led to the documented morphological variation among species in *Artibeus*
593 will help to elucidate the evolution of this successful group of bats.
594
595 **Acknowledgements**
596 I thank Jacob Esselstyn (LSU) for access to specimens and help in the Louisiana State University
597 Museum of Natural History collections. I thank Sam Cordero, Andrea D. Rummel (Brown
598 Univ.), V. David Munteanu (Clemson Univ.), and Samantha L. Cox (Univ. of Penn) for
599 comments and insights on earlier versions of this manuscript. I thank Ilse Garcia Romero and
600 Liliana Dávalos (Stony Brook University) for writing and editing the Spanish language abstract.
601 Finally, I thank Daniel Silva (editor), Kara Powder, Fabio Machado, and three anonymous
602 reviewers for reviews that have greatly improved this manuscript.
603
604 **References**
605

606 **Adams DC, Otárola-Castillo E. 2013.** geomorph: an R package for the collection and analysis
607   of geometric morphometric shape data. *Methods in Ecology and Evolution* **4**:393–399.
608 **Arita HT, Fenton MB. 1997.** Flight and echolocation in the ecology and evolution of bats.
609   *Trends in Ecology and Evolution* **12**:53–58.

610   **August PV. 1981.** Fig fruit consumption and seed dispersal by *Artibeus jamaicensis* in the
611   Llanos of Venezuela. *Biotropica* **13**:70–76.
612   **Balseiro F, Mancina CA, Guerrero JA. 2009.** Taxonomic status of *Artibeus anthonyi*
613   (Chiroptera: Phyllostomidae), a fossil bat from Cuba. *Journal of Mammalogy* **90**:1487–
614   1494.
615   **Bates JM, Hackett SJ, Cracraft J. 1998.** Area-relationships in the Neotropical lowlands: an
616   hypothesis based on raw distributions of passerine birds. *Journal of Biogeography*
617   **25**:783-793.
618   **Bookstein FL. 1997.** Morphometric tools for landmark data: geometry and biology: Cambridge
619   University Press.
620   **Brosset A, Charles-Dominique P. 1990.** The bats from French Guiana: a taxonomic, faunistic
621   and ecological approach. *Mammalia* **54**:509–560.
622   **Burgin CJ, Colella JP, Kahn PL, Upham NS. 2018.** How many species of mammals are there?
623   *Journal of Mammalogy* **99**:1–14.
624   **Collyer ML, Sekora DJ, Adams DC. 2015.** A method for analysis of phenotypic change for
625   phenotypes described by high-dimensional data. *Heredity* **115**:357–365.
626   **Chown SL, Gaston KJ. 2010.** Body size variation in insects: a macroecological perspective.
627   *Biological Reviews* **85**:139–169.
628   **Dumont ER. 1999.** The effect of food hardness on feeding behaviour in frugivorous bats
629   (Phyllostomidae): an experimental study. *Journal of Zoology* **248**:219–229.
630   **Dumont ER., O'Neal R. 2004.** Food hardness and feeding behavior in Old World fruit bats
631   (Pteropodidae). *Journal of Mammalogy* **85**:8–14.
632   **Dumont ER, Davalos LM, Goldberg A, Santana SE, Rex K, Voigt CC. 2012.** Morphological
633   innovation, diversification and invasion of a new adaptive zone. *Proceedings of the Royal*
634   *Society B: Biological Sciences* **279**:1797–1805.
635   **Dumont ER, Samadevam K, Grosse I, Warsi OM, Baird B, Davalos LM. 2014.** Selection for
636   mechanical advantage underlies multiple cranial optima in new world leaf-nosed bats.
637   *Evolution* **68**:1436–1449.
638   **Eisenberg JF, Redford KH. 1989.** Mammals of the Neotropics, Volume 3: Ecuador, Bolivia,
639   Brazil: University of Chicago Press.
640   **Ferreira WAS, Borges BdN, Rodrigues-Antunes S, Andrade FAGd, Aguiar GFdS, Silva-**
641   **Junior JdSe, Marques-Aguiar SA, Harada ML. 2014.** Phylogeography of the dark
642   fruit-eating bat *Artibeus obscurus* in the Brazilian Amazon. *Journal of Heredity* **105**:48–
643   59.
644   **Fleming TH. 1986**. Opportunism versus specialization: the evolution of feeding strategies in
645   frugivorous bats. Frugivores and seed dispersal: Springer, 105–118.
646   **Freeman PW. 2000.** Macroevolution in Microchiroptera: recoupling morphology and ecology
647   with phylogeny. Mammalogy Papers: University of Nebraska State Museum:8.
648   **Galetti M, Morellato L. 1994.** Diet of the large fruit-eating bat *Artibeus lituratus* in a forest
649   fragment in Brasil. *Mammalia* **58**:661–664.
650   **Guerrero JA, De Luna E, Sánchez-Hernández C. 2003**. Morphometrics in the quantification
651   of character state identity for the assessment of primary homology: an analysis of
652   character variation of the genus *Artibeus* (Chiroptera: Phyllostomidae). *Biological*
653   *Journal of the Linnean Society* **80**:45–55.

654 **Hedrick BP, Cordero SA, Zanno LE, Noto C, Dodson P. 2019**. Quantifying shape and
655   ecology in avian pedal claws: The relationship between the bony core and keratinous
656   sheath. *Ecology and Evolution* **9**:11545–11556.
657 **Hedrick BP, Dickson BV, Dumont ER, Pierce SE. 2020.** The evolutionary diversity of
658   locomotor innovation in rodents is not linked to proximal limb morphology. *Scientific*
659   *Reports* **10**:1–11.
660 **Hedrick BP, Dumont ER. 2018.** Putting the leaf-nosed bats in context: a geometric
661   morphometric analysis of three of the largest families of bats. *Journal of Mammalogy*
662   **99**:1042–1054.
663 **Hedrick BP, Mutumi GL, Munteanu VD, Sadier A, Davies KT, Rossiter SJ, Sears KE,**
664   **Dávalos LM, Dumont E. 2019.** Morphological diversification under high integration in a
665   hyper diverse mammal clade. *Journal of Mammalian Evolution*:1–13.
666 **James FC. 1970.** Geographic size variation in birds and its relationship to climate. *Ecology*
667   **51**:365–390.
668 **Jones KE, Bininda-Emonds OR, Gittleman JL. 2005.** Bats, clocks, and rocks: diversification
669   patterns in Chiroptera. *Evolution* **59**:2243–2255.
670 **Kay EH, Hoekstra HE. 2008.** Rodents. *Current Biology* **18**:R406–410.
671 **Koch PL. 1986.** Clinal geographic variation in mammals: implications for the study of
672   chronoclines. *Paleobiology* **12**:269–281.
673 **Kunz TH, Diaz CA. 1995.** Folivory in fruit-eating bats, with new evidence from *Artibeus*
674   *jamaicensis* (Chiroptera: Phyllostomidae). *Biotropica* **27**:106–120.
675 **Larsen PA, Marchán-Rivadeneira MR, Baker RJ. 2010.** Natural hybridization generates
676   mammalian lineage with species characteristics. *Proceedings of the National Academy of*
677   *Sciences* **107**:11447–11452.
678 **Lim BK. 1997.** Morphometric differentiation and species status of the Allopatric fruit-eating
679   bats *Artibeus jamaicensis* and *A. planirostris* in Venezuela. *Studies on Neotropical Fauna*
680   *and Environment* **32**:65–71.
681 **Lim BK, Engstrom MD, Patton JC, Bickham JW. 2008.** Systematic review of small fruit-
682   eating bats (*Artibeus*) from the Guianas, and a re-evaluation of *A. glaucus bogotensis*.
683   *Acta Chiropterologica* **10**:243–256.
684 **Machado FA, Zahn TMG, Marroig G. 2018.** Evolution of morphological integration in the
685   skull of Carnivora (Mammalia): Changes in Canidae lead to increased evolutionary
686   potential of facial traits. Evolution **72**:1399–1419.
687 **Marchan-Rivadeneira MR, Larsen PA, Phillips CJ, Strauss RE, Baker RJ. 2012.** On the
688   association between environmental gradients and skull size variation in the great fruit-
689   eating bat, *Artibeus lituratus* (Chiroptera: Phyllostomidae). *Biological Journal of the*
690   *Linnean Society* **105**:623–634.
691 **Marchán-Rivadeneira MR, Phillips CJ, Strauss RE, Guerrero JA, Mancina CA, Baker RJ.**
692   **2010.** Cranial differentiation of fruit-eating bats (genus *Artibeus*) based on size-
693   standardized data. *Acta Chiropterologica* **12**:143–154.
694 **Morales AE, Ruedi M, Field K, Carstens BC. 2019**. Diversification rates have no effect on the
695   convergent evolution of foraging strategies in the most speciose genus of bats, *Myotis*.
696   *Evolution* **73**:2263–2280.
697 **Moore TY, Organ CL, Edwards SV, Biewener AA, Tabin CJ, Jenkins Jr FA, Cooper KL.**
698   **2015.** Multiple phylogenetically distinct events shaped the evolution of limb skeletal
699   morphologies associated with bipedalism in the jerboas. *Current Biology* **25**:2785–2794.

700 **Morrison DW. 1979.** Apparent male defense of tree hollows in the fruit bat, *Artibeus*
701   *jamaicensis*. *Journal of Mammalogy* **60**:11–15.
702 **Morrison DW, Morrison SH. 1981.** Economics of harem maintenance by a neotropical bat.
703   *Ecology* **62**:864–866.
704 **Mutanen M, Pretorius E. 2007**. Subjective visual evaluation vs. tradition and geometric
705   morphometrics in species delimitation: a comparison of moth genitalia. *Systematic*
706   *Entomology* **32**:371–386.
707 **Nagorsen D, Tamsitt J. 1981.** Systematics of *Anoura cultrata*, *A. brevirostrum*, and *A.*
708   *werckleae*. *Journal of Mammalogy* **62**:82–100.
709 **Nogueira MR, Peracchi AL, Monteiro LR. 2009.** Morphological correlates of bite force and
710   diet in the skull and mandible of phyllostomid bats. *Functional Ecology* **23**:715–723.
711 **Ortega J, Castro-Arellano I. 2001.** *Artibeus jamaicensis*. *Mammalian Species*:1–9.
712 **Owen J, Schmidly D, Davis W. 1984.** A morphometric analysis of three species of *Carollia*
713   (Chiroptera, Glossophaginae) from Middle America. *Mammalia* **48**:85–94.
714 **Perez SI, Bernal V, Gonzalez PN. 2006.** Differences between sliding semi-landmark methods
715   in geometric morphometrics, with an application to human craniofacial and dental
716   variation. *Journal of Anatomy* **208**:769–784.
717 **R Core Development Team. 2019.** R: A language and environment for statistical computing. R
718   Foundation for Statistical Computing, Vienna, Austria.
719 **Redondo RA, Brina LP, Silva RF, Ditchfield AD, Santos FR. 2008.** Molecular systematics of
720   the genus *Artibeus* (Chiroptera: Phyllostomidae). *Molecular Phylogenetics and Evolution*
721   **49**:44–58.
722 **Rohlf F. 2006.** tpsDig, version 2.10. http://life bio sunysb edu/morph/index html.
723 **Rojas D, Warsi OM, Dávalos LM. 2016.** Bats (Chiroptera: Noctilionoidea) challenge a recent
724   origin of extant neotropical diversity. *Systematic Biology* **65**:432–448.
725 **Samuels JX, Van Valkenburgh B. 2008.** Skeletal indicators of locomotor adaptations in living
726   and extinct rodents. *Journal of Morphology* **269**:1387–1411.
727 **Santana SE, Dumont ER, Davis JL. 2010.** Mechanics of bite force production and its
728   relationship to diet in bats. *Functional Ecology* **24**:776–784.
729 **Santana SE, Lofgren S. 2013.** Does nasal echolocation influence the modularity of the mammal
730   skull? *Journal of Evolutionary Biology* **26**:2520–2526.
731 **Shi JJ, Rabosky DL. 2015.** Speciation dynamics during the global radiation of extant bats.
732   *Evolution* **69**:1528–1545.
733 **Simmons NB, Voss RS. 1998.** The mammals of Paracou, French Guiana, a Neotropical lowland
734   rainforest fauna. Part 1, Bats. *Bulletin of the AMNH*:237.
735 **Sneath PH, Sokal RR. 1973.** Numerical taxonomy. The principles and practice of numerical
736   classification.
737 **Stevens RD, Johnson ME, McCulloch ES. 2016.** Geographic variation of wing morphology of
738   great fruit-eating bats (*Artibeus lituratus*): environmental, genetic and spatial correlates
739   of phenotypic differences. *Biological Journal of the Linnean Society* **118**:734–744.
740 **Storz JF, Balasingh J, Bhat HR, Nathan PT, Doss DPS, Prakash AA, Kunz TH. 2001.** Clinal
741   variation in body size and sexual dimorphism in an Indian fruit bat, *Cynopterus sphinx*
742   (Chiroptera: Pteropodidae). *Biological Journal of the Linnean Society* **72**:17–31.
743 **Swanson HK, Lysy M, Power M, Stasko AD, Johnson JD, Reist JD. 2015**. A new
744   probabilistic method for quantifying n-dimensional ecological niches and niche overlap.
745   *Ecology* **96**:318–324.

746 **Vander Linden A, Hedrick BP, Kamilar JM, Dumont ER. 2019.** Atlas morphology, scaling
747   and locomotor behaviour in primates, rodents and relatives (Mammalia:
748   Euarchontoglires). *Zoological Journal of the Linnean Society* **185**:283–299.
749 **Williams DF, Findley JS. 1979**. Sexual size dimorphism in vespertilionid bats. *The American
750   Midland Naturalist* **102**:113–126.
751 **Zelditch ML, Swiderski DL, Sheets HD. 2012.** Geometric morphometrics for biologists: a
752   primer: Academic Press.
753 **Zortea M, Mendes SL. 1993.** Folivory in the big fruit-eating bat, *Artibeus lituratus* (Chiroptera:
754   Phyllostomidae) in eastern Brazil. *Journal of Tropical Ecology* **9**:117–120.
755
756

757   **Tables:**

758

759   **Table 1:** Lateral view Procrustes ANOVA assessing the relationship between shape, species, sex,

760   and log10-transformed centroid size (Shape ~ Species * Sex * Size). Bolded values represent

761   significant p-values at $\alpha = 0.05$. Df – degrees of freedom. SS – sum of squares. MS – mean

762   squares.

763

764   **Table 2:** Ventral view Procrustes ANOVA assessing the relationship between shape, species, sex,

765   and log10-transformed centroid size (Shape ~ Species * Sex * Size). Bolded values represent

766   significant p-values at $\alpha = 0.05$. Df – degrees of freedom. SS – sum of squares. MS – mean

767   squares.

768

769   **Table 3:** Pairwise comparison p-values between countries for the *A. lituratus* data (lateral view

770   above diagonal, ventral view below diagonal). (Shape ~ Sex + Size + Country). Arg = Argentina,

771   Bel = Belize, Cos = Costa Rica, Col = Mexico, Colima, Tab = Mexico, Tabasco, Par = Paraguay,

772   Per = Peru, Tri = Trinidad. Bolded values represent significant p-values at $\alpha = 0.05$. Z-scores are

773   presented in Table S6 for both lateral and ventral views.

774

775   **Table 4:** Average centroid sizes for *A. lituratus* specimens by country with smallest values at the

776   top and largest at the bottom. The order for the lateral view and ventral view is identical.

777

778

779

780

781   **Figure Captions:**
782
783   **Figure 1: Phylogeny of the *Artibeus* species complex.** Representative skulls shown in lateral
784   view with scale bars. Scale = 50 mm. Each skull has its respective species code used in figures 3
785   and 4 (e.g., Aj = *Artibeus jamaicensis*). Colored shapes correspond to species in figures 3 and 4.
786   Large *Artibeus* are represented by triangles and small *Artibeus* are represented by circles. The
787   phylogeny was generated based on Rojas et al. (2016).
788
789   **Figure 2: Landmark configuration for specimens in (A) lateral and (B) ventral views.**
790   Numbered circles correspond to landmarks while red lines correspond to evenly spaced semi-
791   landmark curves. See Table S1 for landmark definitions. Scale = 50 mm.
792
793   **Figure 3: Principal component analyses of the *Artibeus* species complex in (A) lateral view**
794   **and (B) ventral view.** Thin-plate spline grids represent shape change along principal component
795   1 and 2. Colors and species codes refer to individual taxa within the *Artibeus* species complex
796   and are derived from figure 1.
797
798   **Figure 4: Evolutionary allometric trajectories for specimens of the *Artibeus* species**
799   **complex in (A) lateral view and (C) ventral view.** These plots show the common allometric
800   component (CAC) of shape (y-axis) plotted against the log10-transformed centroid size (x-axis).
801   **Centroid size violin plots for (B) lateral view and (D) ventral view.** Colors and species codes
802   refer to individual taxa within the *Artibeus* species complex and are derived from figure 1.
803
804   **Figure 5: Map of Mexico, Central, and South America highlighting countries where**
805   **samples of *A. lituratus* were taken.** Representative skulls shown in lateral view with scale bars.
806   Scale = 50 mm. Colored circles around skulls and countries correspond to colors used to identify
807   countries in figure 6.
808
809   **Figure 6: Principal component analyses for *A. lituratus* subset in (A) lateral view and (C)**
810   **ventral view. UPGMA cluster plots for (B) lateral view and (D) ventral view.** Colors refer to
811   countries where *A. lituratus* specimens were collected and are derived from figure 5. Southern
812   localities (Argentina, Paraguay, Peru, Trinidad) are inverted triangles while northern localities
813   (Mexico, Belize, Costa Rica) are squares.
814
815   **Figure 7: Comparison of male and female shape and size in lateral (A, C) and ventral (B,**
816   **D) views**. For shape wireframes, males are gray and females are black. Wireframes are
817   magnified by three times to accentuate differences, though these differences are quite minor in
818   general.
819

820   Table S1: Landmark definitions. Landmark number, type (according to Bookstein's topology of
821   landmarks), and a description of the landmark in anatomical terms.
822
823   Table S2: Interspecific data including taxon name, specimen number, locality, sex, principal
824   component scores for PC1–4 in lateral and ventral views, centroid sizes in lateral and ventral
825   views, and common allometric coefficient scores in lateral and ventral views.
826
827   Table S3: Interspecific statistical analyses. Results for lateral and ventral view Procrustes
828   ANOVAs of shape and size; shape, species, sex, and size; and size, species, and sex. Tests of
829   phylogenetic signal in lateral and ventral view for shape and size.
830
831   Table S4: Interspecific data for species means used in phylogenetic signal analyses including
832   species names, centroid sizes, and PC1–4 scores for lateral and ventral view.
833
834   Table S5: Intraspecific data for *A. lituratus* including specimen number, locality, sex, country of
835   origin, principal component scores for PC1–4 in lateral and ventral views, and centroid sizes in
836   lateral and ventral views.
837
838   Table S6: Intraspecific statistical analyses for *A. lituratus*. Results for lateral and ventral view
839   Procrustes ANOVAs of shape, sex, size, and country with pairwise comparisons. Distance
840   matrices for country means, and the cophenetic coefficients for lateral and ventral datasets are
841   also included.
842
843   **Figure S1: Principal component analyses of the (A) lateral and (B) ventral views showing**
844   **multiple replicates of one specimen.** To assess error in the data, one specimen was selected at
845   random and landmarked 10 times. That specimen (red) was then plotted in PC morphospace with
846   all other specimens (gray) demonstrating minimal within individual landmarking error compared
847   to between individual differences.
848
849   **Figure S2: Colorblind friendly principal component analyses of the *Artibeus* species**
850   **complex in (A) lateral view and (B) ventral view.** Thin-plate spline grids represent shape
851   change along principal component 1 and 2. Shapes and species codes refer to individual taxa
852   within the *Artibeus* species complex. Species codes refer to figure 1 and shapes are shown next
853   to species codes within the figure.
854
855   **Figure S3: Niche overlap results for the lateral dataset.** X-axis shows the probability (1–100)
856   of niche overlap of the species in the row versus the species in the column. The solid vertical
857   turquoise line represents the mean probability and the hashed vertical turquoise lines represent
858   the 95% confidence intervals. For species pairs where the mean is 0, there is no overlap between
859   species. Aan = *Artibeus anderseni*, Aaz = *A. aztecus*, Aci = *A. cinereus*, Afi = *A. fimbriatus*, Afr
860   = A. *fraterculus*, Aj = *A. jamaicensis*, Al = *A. lituratus*, Ao = *A. obscurus*, Aph = *A. phaeotis*,
861   Apl = *A. planirostris*, At = *A. toltecus*.
862
863   **Figure S4: Niche overlap results for the ventral dataset.** X-axis shows the probability (1–100)
864   of niche overlap of the species in the row versus the species in the column. The solid vertical
865   turquoise line represents the mean probability and the hashed vertical turquoise lines represent

866 the 95% confidence intervals. For species pairs where the mean is 0, there is no overlap between
867 species. Aan = *Artibeus anderseni*, Aaz = *A. aztecus*, Aci = *A. cinereus*, Afi = *A. fimbriatus*, Afr
868 = A. *fraterculus*, Aj = *A. jamaicensis*, Al = *A. lituratus*, Ao = *A. obscurus*, Aph = *A. phaeotis*,
869 Apl = *A. planirostris*, At = *A. toltecus*.
870
871 **Figure S5: Phylomorphospace and disparity through time**. Principal component
872 morphospaces (PC1 x PC2) for species means in (A) lateral and (B) ventral views with the
873 species phylogeny from Rojas et al. (2016) plotted on top of points. White circles represent
874 nodes on the phylogeny. Colors correspond to species colors in figure 1 of the main text.
875 Disparity through time analyses for (C) lateral and (D) ventral views. Solid line represents
876 observed data while dotted line represents Brownian motion. Both views show an increase in
877 disparity at ~5 mya at the split between the small and large *Artibeus*.
878
879 File S1: TPS file for interspecific dataset in lateral view.
880
881 File S2: TPS file for interspecific dataset in ventral view.
882
883 File S3: TPS file for intraspecific dataset (just *A. lituratus*) in lateral view.
884
885 File S4: TPS file for intraspecific dataset (just *A. lituratus*) in ventral view.
886
887

Figure 1

Figure 1: Phylogeny of the *Artibeus* species complex.

Representative skulls shown in lateral view with scale bars. Scale = 50 mm. Each skull has its respective species code used in figures 3 and 4 (e.g., Aj = *Artibeus jamaicensis*). Colored shapes correspond to species in figures 3 and 4. Large *Artibeus* are represented by triangles and small *Artibeus* are represented by circles. The phylogeny was generated based on Rojas et al. (2016).
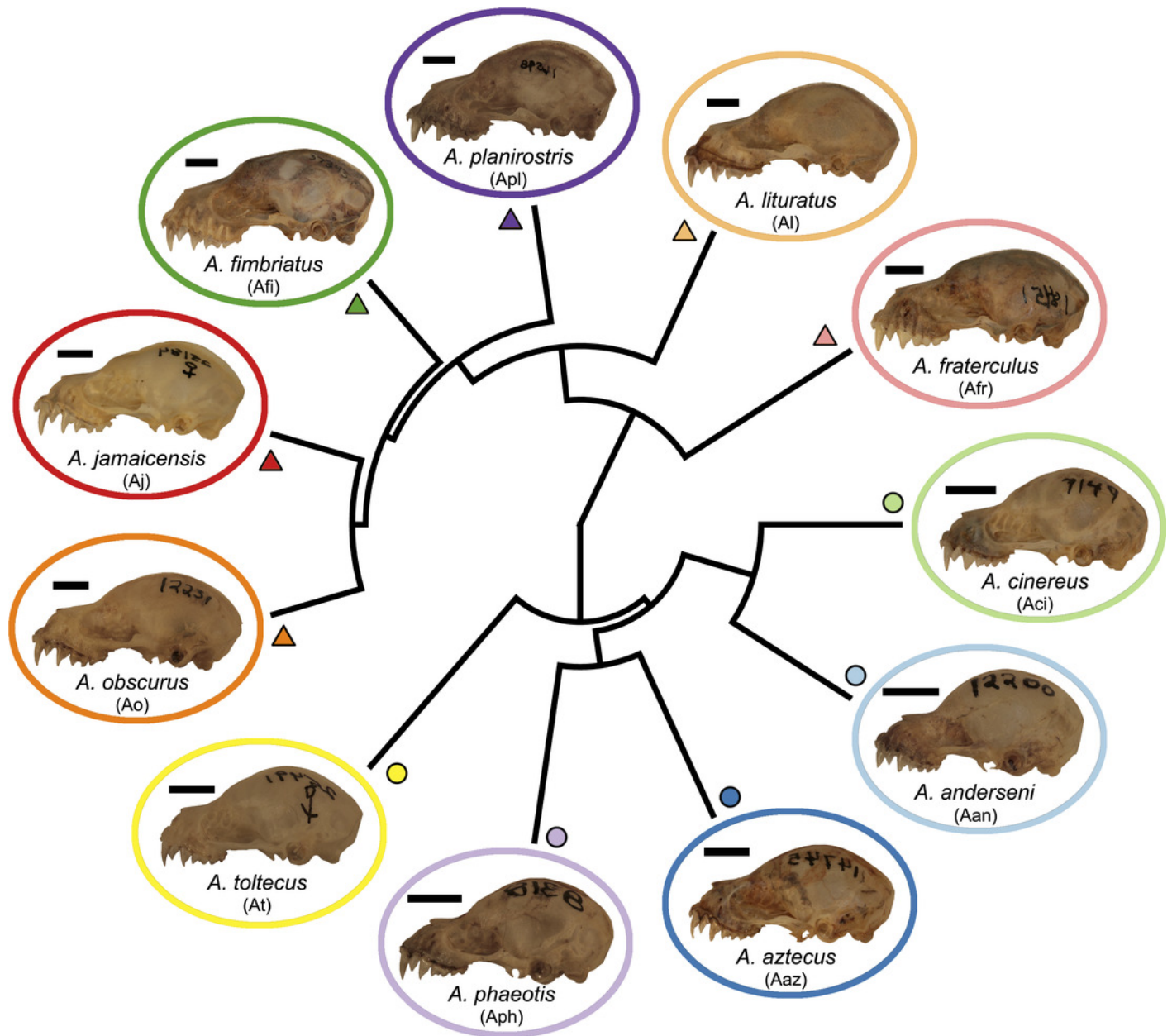
Figure 2

Figure 2: Landmark configuration for specimens in (A) lateral and (B) ventral views.

Numbered circles correspond to landmarks while red lines correspond to semi-landmark curves. See Table S1 for landmark definitions. Scale = 50 mm.
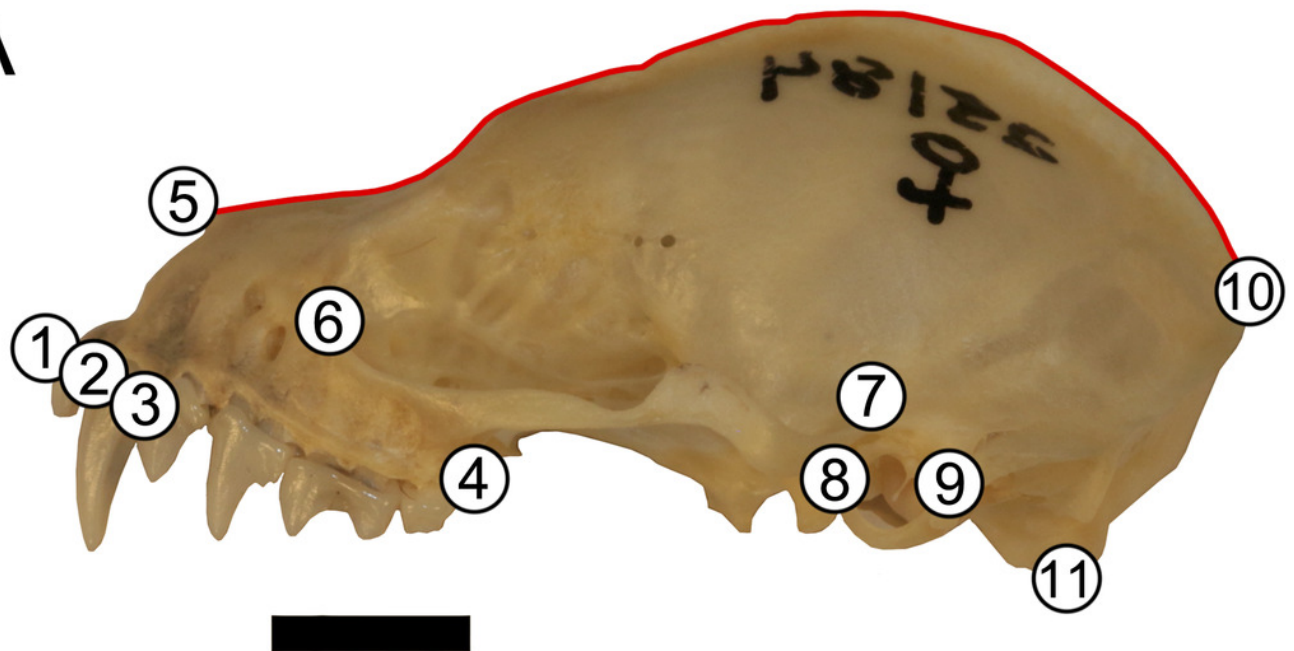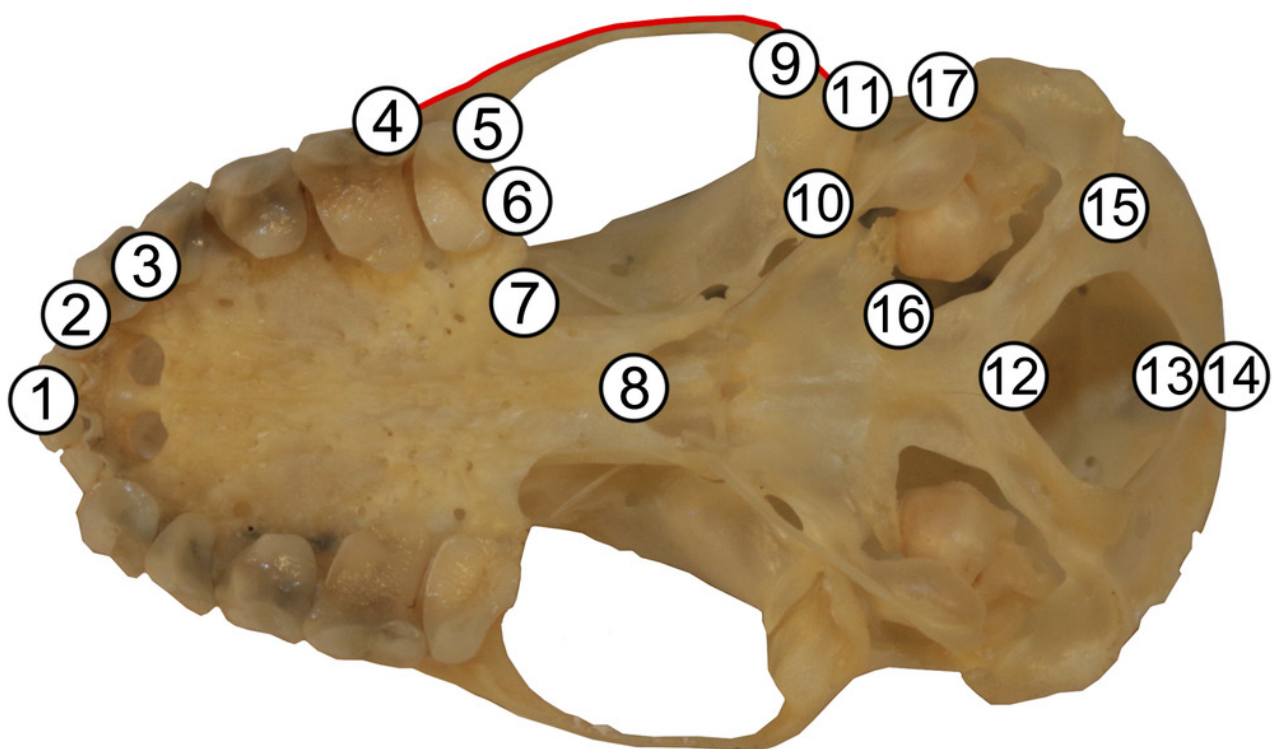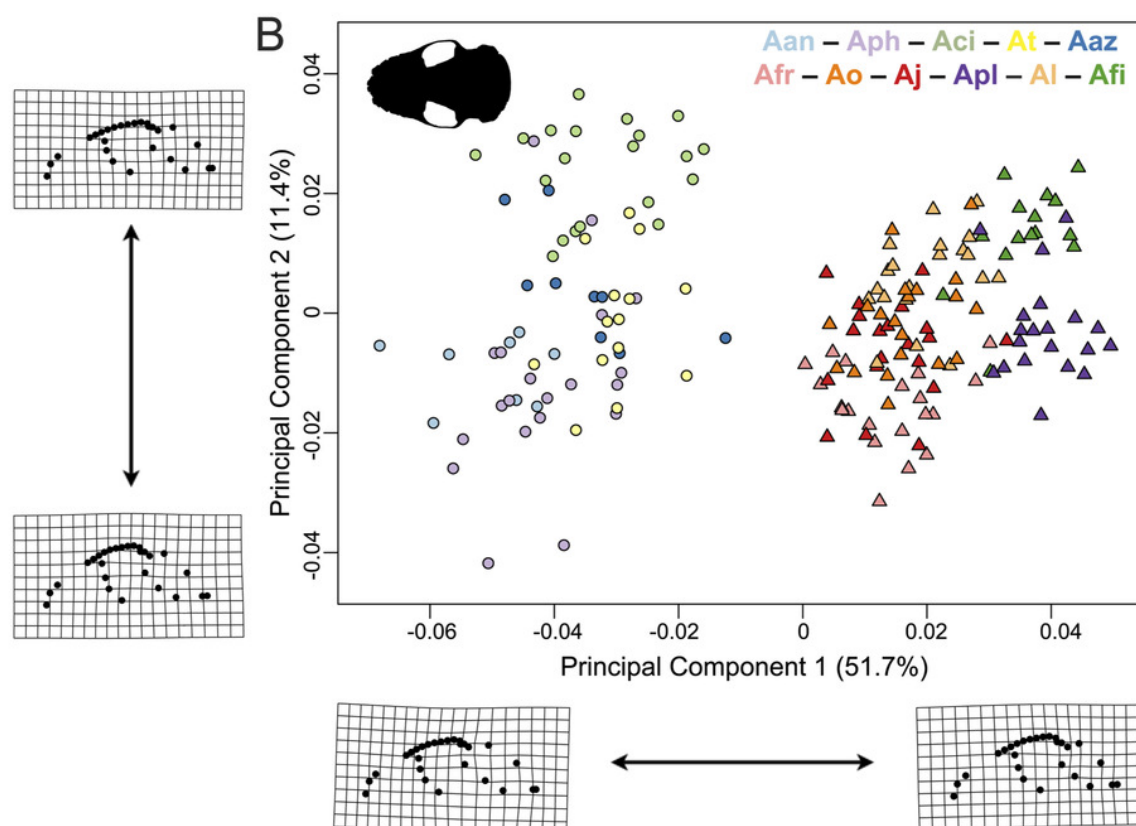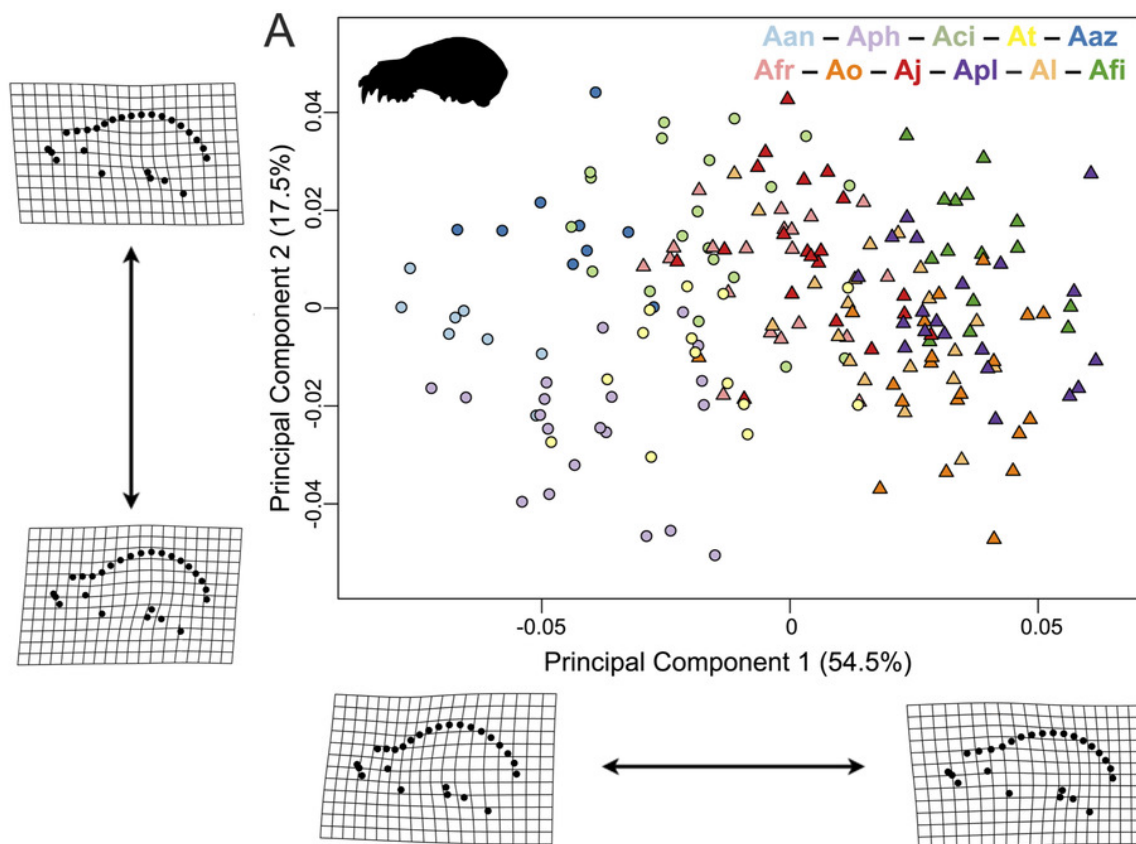
Figure 4

Figure 4: Evolutionary allometric trajectories for specimens of the *Artibeus* species complex in (A) lateral view and (C) ventral view.

These plots show the common allometric component (CAC) of shape (y-axis) plotted against the log10-transformed centroid size (x-axis). **Centroid size box plots for (B) lateral view and (D) ventral view.** Colors and species codes refer to individual taxa within the *Artibeus* species complex and are derived from figure 1.
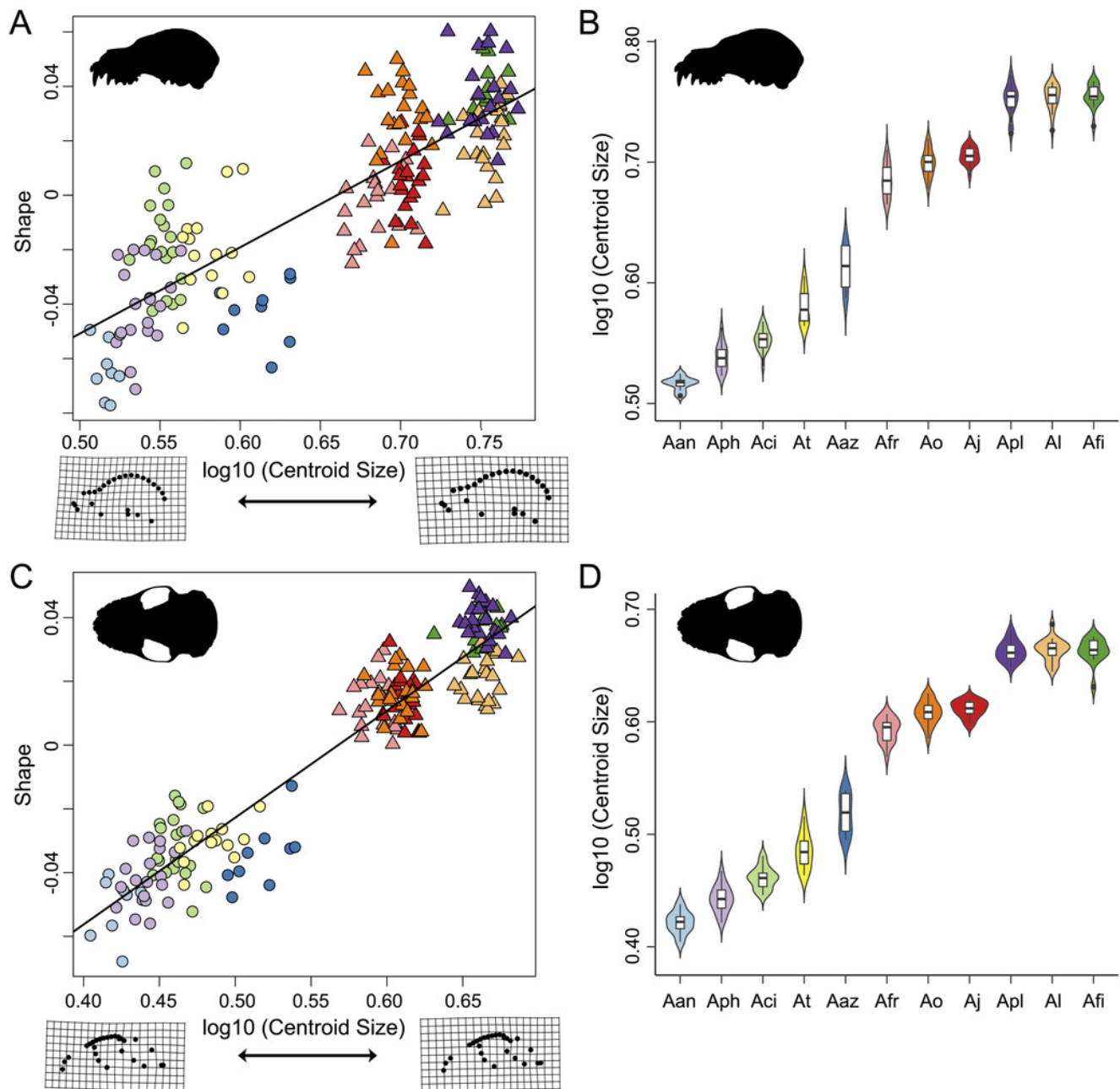
Figure 5

Figure 5: Map of Mexico, Central, and South America highlighting countries where samples of *A. lituratus* were taken.

Representative skulls shown in lateral view with scale bars. Scale = 50 mm. Colored circles around skulls and countries correspond to colors used to identify countries in figure 6.
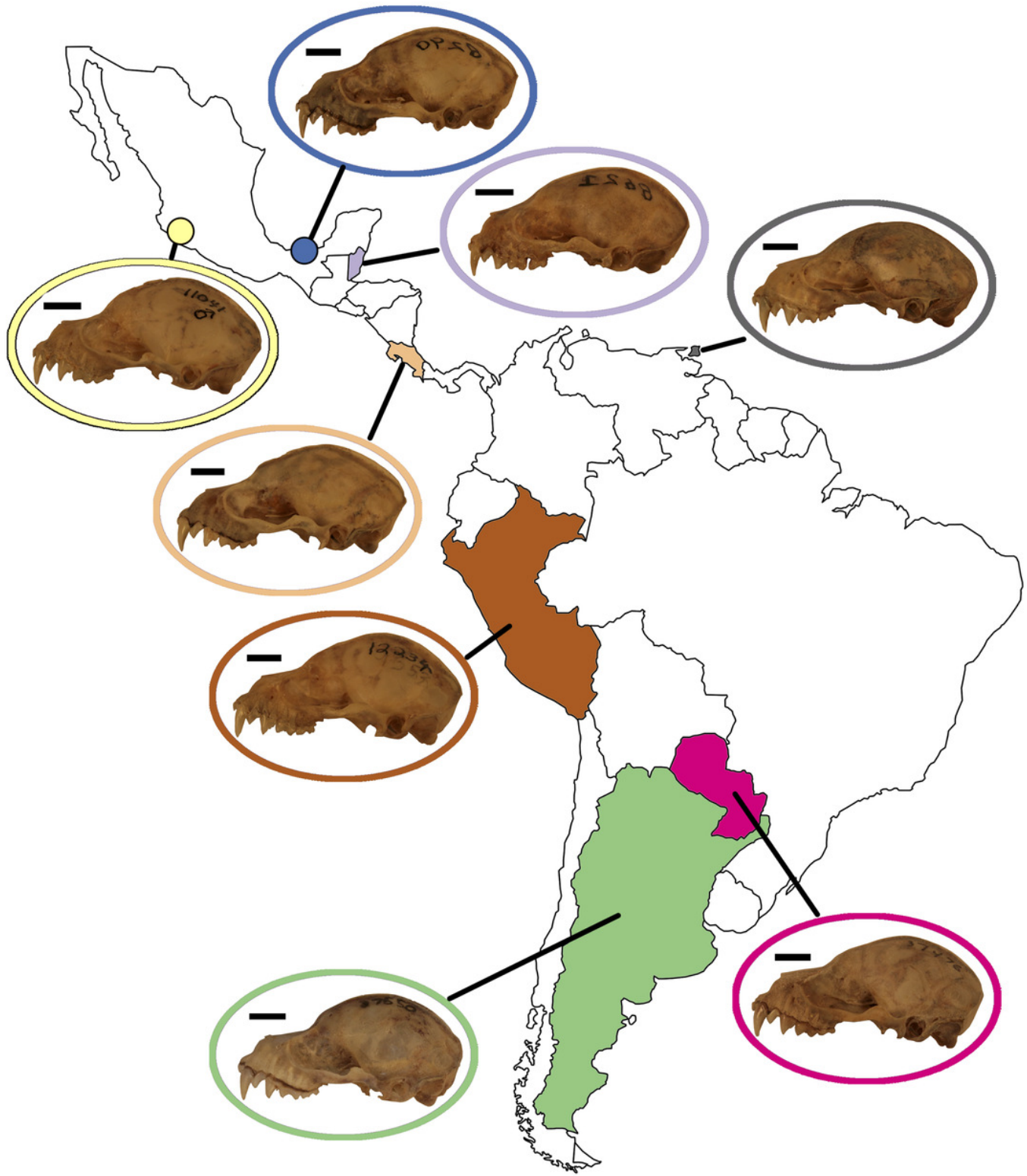
Figure 6

Figure 6: Principal component analyses for *A. lituratus* subset in (A) lateral view and (C) ventral view. UPGMA cluster plots for (B) lateral view and (D) ventral view.

Colors refer to countries where *A. lituratus* specimens were collected and are derived from figure 5. Southern localities (Argentina, Paraguay, Peru, Trinidad) are inverted triangles while northern localities (Mexico, Belize, Costa Rica) are squares.
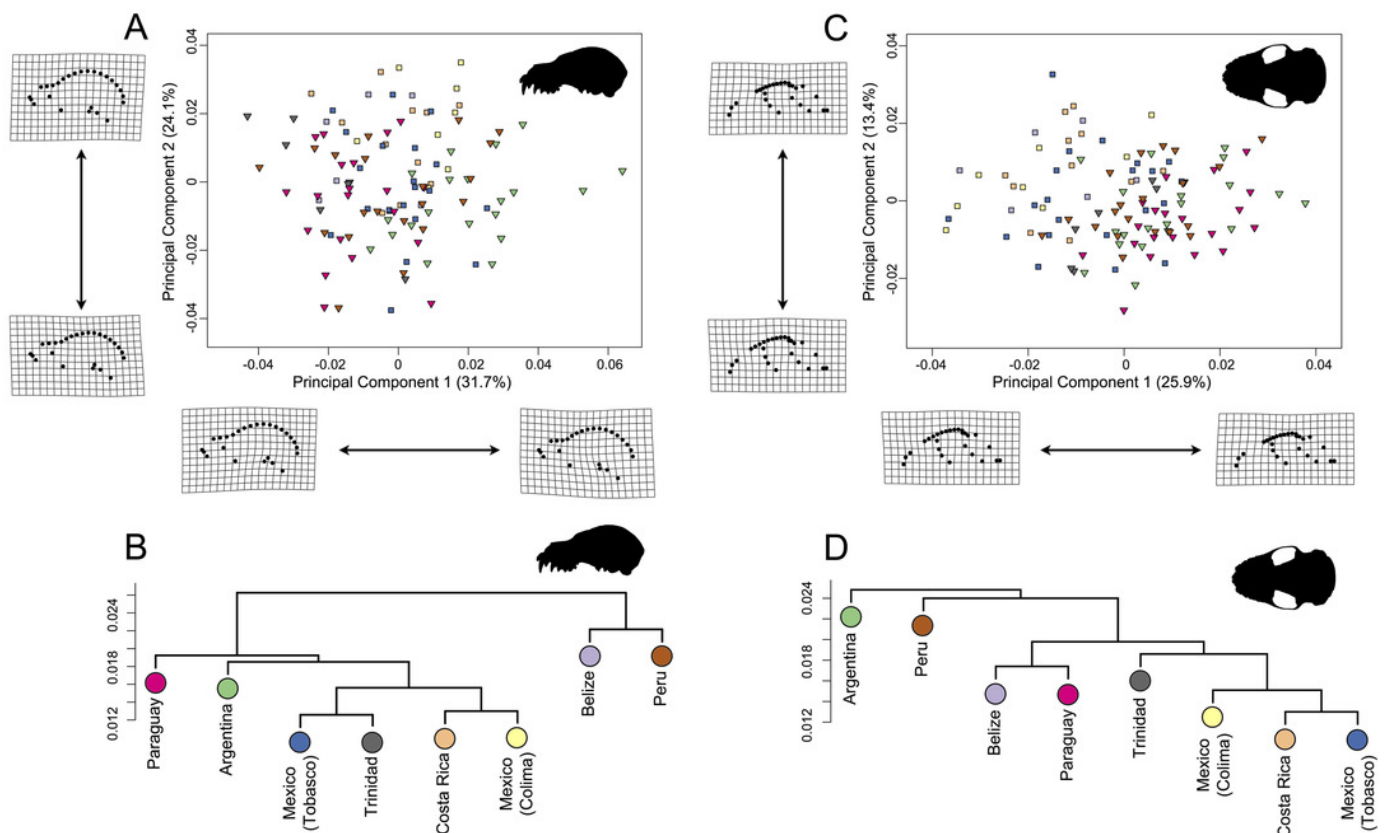
Figure 7

Figure 7: Comparison of male and female shape and size in lateral (A, C) and ventral (B, D) views.

For shape wireframes, males are gray and females are black. Wireframes are magnified by three times to accentuate differences, though these differences are quite minor in general.

Lateral view Procrustes ANOVA assessing the relationship between shape, species, sex, and log10-transformed centroid size (Shape ~ Species * Sex * Size). Bolded values represent significant p-values at a = 0.05. Df – degrees of freedom. SS – sum of square

1 **Table 1:** Lateral view Procrustes ANOVA assessing the relationship between shape, species,
2 sex, and log10-transformed centroid size (Shape ~ Species * Sex * Size). Bolded values
3 represent significant p-values at $\alpha = 0.05$. Df – degrees of freedom. SS – sum of squares. MS –
4 mean squares.

	Df	SS	MS	R²	F	Z	p
Species	10	0.228	0.023	0.605	28.058	12.092	**0.001**
Sex	1	0.003	0.003	0.009	4.184	4.654	**0.001**
Size	1	0.004	0.004	0.010	4.521	5.040	**0.001**
Species:Sex	10	0.010	0.001	0.026	1.183	6.596	**0.001**
Species:Size	10	0.010	0.001	0.026	1.197	6.733	**0.001**
Sex:Size	1	0.000	0.000	0.000	0.133	-1.405	0.919
Species:Sex:Size	10	0.007	0.001	0.018	0.841	5.441	**0.001**
Residuals	142	0.115	0.001	0.306			
Total	185	0.377					

Table 2: Ventral view Procrustes ANOVA assessing the relationship between shape, species, sex, and log10-transformed centroid size (Shape ~ Species * Sex * Size). Bolded values represent significant p-values at α = 0.05. Df – degrees of freedom. SS – sum
1 **Table 2:** Ventral view Procrustes ANOVA assessing the relationship between shape, species,
2 sex, and log10-transformed centroid size (Shape ~ Species * Sex * Size). Bolded values
3 represent significant p-values at α = 0.05. Df – degrees of freedom. SS – sum of squares. MS –
4 mean squares.

	Df	SS	MS	R²	F	Z	p
Species	10	0.220	0.022	0.630	31.324	13.058	**0.001**
Sex	1	0.001	0.001	0.002	1.149	3.081	**0.001**
Size	1	0.003	0.003	0.010	4.922	6.701	**0.001**
Species:Sex	10	0.008	0.001	0.023	1.151	9.060	**0.001**
Species:Size	10	0.010	0.001	0.027	1.366	10.198	**0.001**
Sex:Size	1	0.001	0.001	0.002	0.915	3.091	**0.003**
Species:Sex:Size	10	0.007	0.001	0.020	0.970	8.133	**0.001**
Residuals	142	0.100	0.001	0.286			
Total	185	0.350					

Table 3: Pairwise comparison p-values between countries for the *A. lituratus* data (lateral view above diagonal, ventral view below diagonal). (Shape ~ Sex + Size + Country). Arg = Argentina, Bel = Belize, Cos = Costa Rica, Col = Mexico, Colima, Tab

1 **Table 3:** Pairwise comparison p-values between countries for the *A. lituratus* data (lateral view
2 above diagonal, ventral view below diagonal). (Shape ~ Sex + Size + Country). Arg = Argentina,
3 Bel = Belize, Cos = Costa Rica, Col = Mexico, Colima, Tab = Mexico, Tabasco, Par = Paraguay,
4 Per = Peru, Tri = Trinidad. Bolded values represent significant p-values at α = 0.05. Z-scores are
5 presented in Table S6 for both lateral and ventral views.

	Arg	Bel	Cos	Col	Tab	Par	Per	Tri
Arg		**0.001**	**0.001**	**0.001**	**0.001**	**0.001**	**0.001**	**0.001**
Bel	**0.001**		0.257	**0.044**	**0.039**	0.064	**0.035**	0.535
Cos	**0.001**	0.283		0.569	0.079	**0.006**	**0.033**	**0.037**
Col	**0.001**	0.791	0.164		**0.013**	**0.002**	**0.013**	**0.011**
Tab	**0.001**	0.157	0.269	0.084		0.116	0.595	**0.037**
Par	0.096	**0.001**	**0.001**	**0.001**	**0.001**		**0.041**	0.189
Per	0.088	**0.006**	**0.002**	**0.001**	**0.019**	**0.004**		0.016
Tri	0.19	**0.045**	0.108	**0.014**	0.417	**0.035**	0.472	

Table 4: Average centroid sizes for *A. lituratus* specimens by country with smallest values at the top and largest at the bottom. The order for the lateral view and ventral view is identical.

1 **Table 4:** Average centroid sizes for *A. lituratus* specimens by country with smallest values at the
2 top and largest at the bottom. The order for the lateral view and ventral view is identical.

	Average Centroid Size Lateral View	Average Centroid Size Ventral View
Belize	5.27	4.24
Mexico, Colima	5.33	4.33
Costa Rica	5.54	4.48
Mexico, Tabasco	5.55	4.53
Argentina	5.68	4.61
Trinidad	5.72	4.64
Peru	5.73	4.65
Paraguay	5.78	4.69